Sub-part Correspondence by Structural Descriptors of 3D Shapes

Silvia Biasotti Simone Marini * Michela Spagnuolo
Bianca Falcidieno

Istituto di Matematica Applicata e Tecnologie Informatiche, Consiglio Nazionale delle Ricerche, Via De Marini, 6 - 16149 Genova, Italy

Abstract

To fully exploit the valuable knowledge embedded in repositories of digital CAD models, it is crucial to devise search engines capable of expressing high-level and advanced queries, which can effectively support the re-use of CAD models. The retrieval mechanism should be able to return not only global similarity measures among objects, but it should be also coupled with methods for the automatic identification of similar sub-parts in the query and retrieved models, possibly highlighting automatically the object differences.

This paper describes a method for partial shape-matching able to recognize similar sub-parts of objects represented as 3D polygonal meshes. The geometry and the structure of the shapes are coupled in a descriptor that provides a flexible coding, grounded on solid mathematical theories, and that can be adapted to the user's needs and to the context of applications. The matching framework for sub-part correspondence is achieved through a graph-matching technique, which builds the common sub-graphs between the two shapes and highlights the maximal sub-parts having similar structure and similar space distribution.

Key words: shape similarity, sub-part shape correspondence, structural shape descriptor, graph matching

* Corresponding author. Tel.: +39 010 6475 696. Fax.: +39 010 6475 660.
Email addresses: sivia.biasotti@ge.imati.cnr.it (Silvia Biasotti),
simone.marini@ge.imati.cnr.it (Simone Marini),
michela.spagnuolo@ge.imati.cnr.it (Michela Spagnuolo),
bianca.falcidieno@ge.imati.cnr.it (Bianca Falcidieno).

1 Introduction

Technological improvements related to object acquisition, visualization and modeling, have caused a considerable growth of the number of 3D models in digital form, which are now available in large databases of shapes, ranging from unstructured repositories, like the web, to specialized catalogues used in engineering and simulation. Whilst there are already techniques for rapidly extracting knowledge from massive volumes of texts (e.g., Google), it is harder to structure, filter, organize, retrieve and maintain archives of digital shapes. This is especially crucial for CAD model databases which contain designed shapes: it has been estimated, indeed, that a large part of the design activity is based on the reuse of previous knowledge to address new design problems (Ullman, 1997; Regli and Cicirello, 2000; Iyer et al., 2005). Efficient 3D search engines are therefore necessary to avoid re-inventing (or re-designing) the wheel every time, and to support the re-use of design models. To better approach the problem of shape similarity, three aspects should be considered: the first concerns how the similarity is assessed, since an automatic retrieval system should mimic human perception. The second aspect concerns the influence of the application context in the similarity evaluation, and the third is the shape representation, which could be mathematical, symbolic or syntactical.

Human perception has been widely studied and applied especially to computer vision problems (Biederman, 1987; Marr, 1982). There is a large consensus that shapes are recognized and coded mentally in terms of relevant parts and their spatial configuration, or structure. Relevant parts are obviously dependent on the application, meaning that we are able to index an object with different features according to the context in which we are asked to describe it. Moreover, even remaining in the same context of application, the same object could be described with respect to different features. As pointed out by (Bespalov et al., 2005), this is very relevant to the engineering context, where objects could be searched for their functional features that might also not be related to a unique geometric form. This suggests that the first and second aspects are clearly correlated and difficult to be formalized: the way we perceive shapes is strongly influenced by the context and depends on subjective or application-dependent properties.

An important point is that the similarity between two shapes is assessed not only in terms of identical global match but it is based on the contribution of common features compared to those distinguishing them, as for a keyword search in comparing texts. Therefore, a retrieval system closer to the human perception of similarity should be able to assess similarity but also to identify the common parts (*global* and *partial* matching). For engineering applications, partial matching is definitely desirable: if an existing object differs only in a few details from a new model to be produced, then it is not difficult to adapt

(a) (b) (c)

Fig. 1. The shape of these models influences the way they may be used.

the process plan of the existing object to the new one.

These considerations suggest that also the third aspect, i.e. shape representation, should be addressed trying to devise very flexible computational descriptions that store the shape structure with respect to its features, and that can be easily adapted to different contexts. Different approaches to feature characterization have been adopted in the literature, yielding to different shape structuring. The shape characterization is usually asked to be invariant to affine transformations, to guarantee uniqueness of the object description, and may be based on local geometric properties, like curvature, or on fitting a number of pre-defined primitives to the geometric model (Katz et al., 2005; Biederman, 1987).

Structure-based shape description is particularly important for engineering applications. The use of structural descriptors is an intermediate step between the geometry and the semantics of the object, since it characterizes features of the object, relevant with respect to the application context or the design activities, like holes, slots and handles. Information about the shape structure may make the difference when the sub-part analysis supports decisions on how to reuse a mechanical part for the design of a new CAD model. For example, the bearing models in figure 1 have analogous function but their shape influences their context of use: the models (a) and (b) need a washer to be fixed, while the model in (c) admits the usage of nails or screws.

We believe that by differentiating the geometric, structural and semantic level of description of shapes, an automatic retrieval system will be able to provide results closer to the human intuition of similarity. Since there is neither a single *best* shape characterization nor a single *best* similarity measure, we propose a framework for working on shape retrieval where different characterization methods can be plugged-in and tested, while keeping the same computational setting. The majority of the methods developed so far for shape matching span from coarse filters suited to browse large 3D repositories on the web, to domain-specific approaches to assess the similarity of models; they are related to four main scenarios:

(1) recognition of objects whose overall shape is similar (global matching);
(2) recognition of similar sub-parts in objects that are both structurally and globally similar (sub-part correspondence);
(3) recognition of similar sub-parts in objects having different overall shape (partial matching);
(4) recognition of a whole object as a sub-part of another (part-in-whole).

Note that the fourth case is a particular case of the third one. The majority of the methods developed so far for shape matching fit into the first category, and span from coarse filters suited to browse large 3D repositories on the web, to domain-specific approaches to assess the similarity of models. Most of the methods are based on geometric shape descriptors (e.g., distances, angles, curvatures, area, or volumes) which characterize the shape distribution of the object in the 3D space (Vranič et al., 2001; Novotni and Klein, 2001; Osada et al., 2001; Kazhdan et al., 2003) . These methods are suited to solve the global matching problem, and the matching is measured by some function that provides a global value of similarity. In this sense, they do not have the capability to explicitly represent the relevant sub-parts of the object and how this sub-part are spatially related among them. Methods for sub-part correspondence and for partial matching are more elaborate in the sense that they provide not only a global measure of similarity, but also the indication of where the similarities occur in the shapes. A brief review of this class will be given in Section 2.

1.1 Paper contribution

This paper contributes to all facets of the partial correspondence problem with major emphasis on the second one, due to the properties of the adopted structural descriptor. The geometry and the structure are coupled for identifying the maximal sub-parts having similar structure and similar space distribution. The shape description framework provides a flexible coding, grounded on solid mathematical theories, that can be adapted to the user's needs and to the context of applications. In figure 2, an example of the correspondences detected between two mechanical parts is shown. The light-blue parts represent the sub-parts with similar geometry and structure, while the grey ones denote the sub-parts whose shape significantly differs.

The structural shape descriptor that we have chosen in order to validate the approach is based on the theory of Reeb graph, as explained in detail in section 3. The shape and all its relevant sub-parts are encoded in a graph which carries a topological and geometric signature of the shape. This choice allows two degrees of freedom: first, the relevant sub-parts are defined implicitly by the choice of the function that is used to analyze the shape, and second,

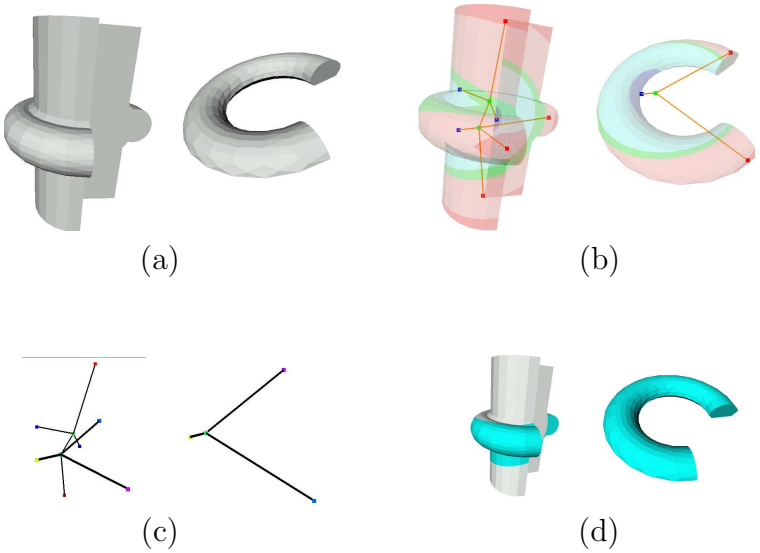

Fig. 2. Two mechanical parts (a) are shown together with their structural descriptors (b). In (c) the matching between the two graphs is represented by the nodes with the same color and by the thicky edges. The sub-part correspondence is represented in (d).

the geometry of the relevant parts can be described by different geometric parameters. In this work, the geometric signature is built using the spherical harmonics defined in (Kazhdan et al., 2003) which are associated to each object sub-parts.

The structural representation can be always coded as a directed graph, and therefore partial matching can be solved by finding a mapping between the sub-graphs of the descriptions. This is achieved through the construction of a common sub-graph (possibly not connected) between the two input graphs, that highlights where two shapes are similar or dissimilar. Graph matching has been used extensively in a variety of applications and by graph matching, or more commonly by inexact subgraph isomorphism, it is possible indeed to assess the similarity among shapes as well as among parts of a shape. Inexact graph matching also ensures the stability of the matching with respect to noise, for example in presence of irrelevant structural differences. The proposed matching framework is able to *modularly* incorporate different heuristic techniques for reducing the computational costs of the graph matching process and for adapting the similarity estimation to the application context for which it is used.

The reminder of the paper is organized as follows. First, a brief discussion on existing techniques for shape retrieval and partial matching is given. Then, the description of the approach is given; since solving the correct graph matching problem is computationally expensive, a new heuristic method which speeds up the process is proposed. Finally, results are presented and discussed. Conclusive remarks and suggestions on future work end the paper.

2 Literature Survey

Most of methods for 3D object comparison are best suited for global matching, because they return as output a positive real number which measures how much an object resembles to another one. Since no information on the sub-part correspondence of the compared objects is stored, these approaches are not available to solve the sub-part correspondence and partial matching problems. However, this information is needed in applications like object modeling, registration and recognition, (Ruiz-Correa et al., 2003; Funkhouser et al., 2004; Huber et al., 2004). In this section some relevant approaches for sub-part correspondence and partial matching problems are discussed.

The method proposed in (Johnson and Hebert, 1997) does not require any feature extraction or segmentation, it samples the object surface into a set of oriented points (3D points with surface normals) and associates to each sampled point a description of the surface around it: the spin-image. A similarity measure between 2D images is used to evaluate the similarity between two spin-images and thus between two oriented points of the compared objects. In this way a point-to-point correspondence between the two objects is provided. In (Ruiz-Correa et al., 2003) the similarity measure defined among spin-images is used to group oriented points into pathces. This approach allows the correspondence between patches instead of points.

Other approaches, like those described in (Fan et al., 1989; Huber et al., 2004; Funkhouser et al., 2004; Bespalov et al., 2003b) represent 3D objects as a set of parts which are compared to obtain an object sub-part mapping.

The use of spin-images for classifying sub-parts of 3D objects has been recently proposed in (Huber et al., 2004). The proposed method has been experimented on 3D models of cars, where each model has been arbitrarily split into three sub-parts (front, middle and rear part of the car), and each sub-part is represented by a collection of spin-images that capture the regional object shape at random locations distributed over the surface part. This method groups car models into classes of similar cars by supposing that sub-parts of cars having similar signatures are expected to have similar overall shape.

The scheme in (Funkhouser et al., 2004), describes a methodology to interactively build new objects by composing sub-parts of existing objects already stored in a database. The steps the user has to perform to build a new model are: choosing a model from the database; selecting a sub-part of the model to be edited: searching in the database for a model with a similar sub-part; selecting one of the models returned by the search and performing the editing operations. The comparison process retrieves objects that have similar overall shape and that are aligned in the same coordinate system. The sub-part cor-

respondence is obtained by recognizing the part of the retrieved model that overlaps the user selected part of the query model.

In (Fan et al., 1989) the surface of an object is described by segmenting it into patches obtained by analyzing shape discontinuities of the object surface, like jump boundaries, limbs and creases. This description is encoded as an attributed graph whose nodes correspond to the surface patches and the edges codify the relations between them. Each patch is discretized into a set of geometric descriptors as the surface area, the average orientation, the average of principal curvatures and the centroid. The comparison of two objects is accomplished through a graph matching process where the node correspondences between the two graphs are obtained by enumerating all possible node pairs and iteratively selecting the pairs of nodes that satisfy a set of pre-defined constraints.

Finally, the methods proposed in (Bespalov et al., 2003b, 2004) represent the shape object as binary tree obtained by recursively subdividing the object into two parts. The similarity measure between two objects is obtained by matching the two trees, where the sub-part correspondence is induced by the node mapping provided by the matching algorithm.

All these methods provide only one and arbitrary description of the object shape, while the framework proposed in this paper is based on the consolidated Reeb graph theory that allows the use of different functions to analyze the shape, each one able to identify different relevant sub-parts of the object. In particular, methods based on the spin-images provide a point-to-point correspondence between the object surfaces and need a, may be not simple, post processing phase to identify an explicit correspondence among relevant sub-parts of the objects. Moreover, the spin-images descriptors do not carry any kind of strucutral and topological information. On the contrary, a simple strucutral information is represented in (Fan et al., 1989; Bespalov et al., 2003b, 2004), but the shape analysis is based on shape discontinuities that are not necessarily present in all the mechanical parts, like in (Fan et al., 1989), or the bi-section decomposition process does not grant that meaningful features are encoded into the binary tree like in the (Bespalov et al., 2004). Furthermore, in both methods the matching process does not grant the identification of meaningfull sub-part correspondence and does not provide the capability to modularly incorporate different heuristics able to adapt the matching to the specific application contexts (e.g. global matching, sub-part correspondence, partial matching). Finally the method proposed in (Funkhouser et al., 2004) is not fully automatic and it is not able to solve the partial matching problem as defined in section 1. Moreover it needs a pose estimation and a registration pre-processing phase to solve the sub-part correspondence and the global matching problems.

3 The Shape Structural Descriptor

The use of structures for shape description has been widely addressed in Computer Graphics and Vision. Probably the best-known structure is the one related to the medial axis transformation, that provides a decomposition of the shape in protrusions detected by spheres of different radius inscribed in the shape, (Blum, 1967). The medial axis nicely simulates the human intuition and it is well-suited for shape matching especially for 2D shapes (Sundar et al., 2003; Siddiqi et al., 2002; Zhang et al., 2005b; Iyer et al., 2005). Several geometric descriptors have been proposed for associating to the nodes of a skeletal graph the description of the related model sub-parts. A minimal solution consists in coding in a vector the *relevance* of the skeletal edges incident in a node (e.g. edge length, diameters and average circumference of the skeleton loops) as proposed in (Sundar et al., 2003; Iyer et al., 2005). Another strategy is use geometric descriptors able to support global comparison of 3D shapes, like the mean curvature histogram (Zhang et al., 2005b).

Methods based on the Reeb graph theory, (Reeb, 1946) are an effective alternative to skeletal methods: intuitively, the Reeb graph describes the shape by storing the evolution of level sets of a given real-valued function associated to the shape. The shape can be represented by a graph which stores slices of the shape, possibly with some geometric attributes. (Hilaga et al., 2001) have used the Reeb graph in a multi-resolution fashion for shape matching, and have associated to each node, i.e. shape slice, the ratio of the area and the length of the model sub-part in the whole model. Similar criteria have been successively used in (Bespalov et al., 2003a) and further enriched by (Tung and Schmitt, 2005), where for each slice the geometric attributes considered are the volume, a statistic measure of the extent and the orientation of the triangles, an estimation of the Koenderink shape index and a statistic of the texture.

3.1 Extended Reeb Graph

Given a surface S and a real, continuous function f defined on it, the Reeb graph of S with respect to the mapping function f is the quotient space of S with respect to the equivalence relationship that collapses each contour level of f into a single point. See (Reeb, 1946; Shinagawa et al., 1991) for further references.

Our *Extended Reeb Graph (ERG)* representation generalizes the definition of Reeb graph to a surface on which a finite set of contour levels $C(S)$ is defined.

Since contours are supposed to be non degenerate (i.e. points or open lines),

they subdivide S into a set of regions bordered by elements of $C(S)$. Then, we define two points $P, Q \in S$ as Reeb-equivalent in an extended sense if they belong to the same region or the same contour, see (Biasotti, 2004) for details. The quotient space obtained from this relation is a discrete space, which we call *Extended Reeb (ER)* quotient space. In figure 3, an example of the ER with respect to the distance from the center of mass is shown for a linkage model. Figure 3(a) highlights how the function f varies on the model: blue regions correspond to minima while red ones represent maxima.

This quotient space is coded in the Extended Reeb Graph as follows: first of all, each region is coded into a node of the graph; then, if two regions share a contour, the nodes corresponding to these regions are connected by an edge. In general, a node will be connected to as many nodes as the number of connected components of the border of the associated region. In figure 3(b-c) it is highlighted how the sequence of points of the quotient space ER represents the arcs and nodes of the ERG.

The edges of the ERG may be oriented according to the monotonicity of the function f , which implies that the ERG is directed and acyclic. Furthermore, each node of the graph identifies a subgraph which is empty only in case of leaf nodes.

Finally, the ERG is further simplified by collapsing all nodes whose number of incoming and outgoing edges is 1, without altering the topological correctness of the coding. After this merging step, the ERG simply consists of nodes representing the regions where the topology of the contour levels varies and the associated connecting edges, see figure 3(d).

The ERG naturally provides a graph representation of the shape that reflects into its coding the invariance properties of the mapping function (Biasotti et al., 2003a). In particular, when it is necessary that the shape description is invariant under some transformation, like rigid motions or affine transformations, it is sufficient to choose a mapping function which is invariant under those transformations. Therefore, the dependence of the graph on the mapping function provides a flexible shape characterization that can easily be tuned according to the user needs. Moreover, the Reeb graph is able to correctly code the topology of a closed surface (Cole-McLaughlin et al., 2003).

3.2 The shape descriptor: coupling the ERG with geometric attributes

The functions used to validate the matching framework proposed in this paper are the distance from the center of mass of the object and the integral geodesic distance $f(v) = \int_{p \in M} g(v, p) dS$, where $g(v, p)$ represents the geodesic distance between v and p, when p varies on M. The latter function was originally

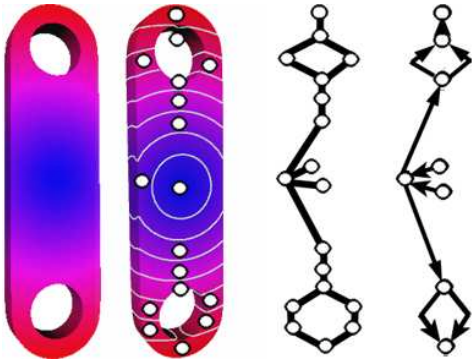

Fig. 3. A model (a), graph nodes that correspond to the regions generated from the contour levels (b), the ERG before (c) and after (d) the simplification of nodes.

proposed in (Hilaga et al., 2001), while variations may be found in (Zhang et al., 2005a; Katz and Tal, 2003). To be suitable for sub-part correspondence issues any other suitable f could be used, provided that it is invariant with respect to object rotation, translation and scaling (Biasotti et al., 2003a,b).

The most important aspect to evaluate when choosing the mapping function is the kind of features that we want to highlight in the description and the type of matching we would like to get. In our example, the distance from the center of mass (barycentre) naturally highlights the distribution of the object with respect to its barycentre. Therefore this function is rotation invariant, but sensitive to pose variations. On the contrary, the function in (Hilaga et al., 2001) is pose invariant because it depends on the shape distribution with respect to the geodesic center of the surface. In both cases, the shape will be described as a configuration of protrusions and hollows, but the geodesic will not discriminate between objects in different poses while the distance from the center of mass will do. Therefore, the geodesic is best suited for retrieving articulated objects disregarding the pose, while the distance from the center of mass will allow to distinguish among articulated models in different poses.

Also computational aspects have to be taken into account when choosing a mapping function. For example, the center of mass may be computed in linear time with respect to the number of vertices and, since it depends on all surface vertices, it is robust to noise. On the contrary, the exact computation of the integral geodesic function may be performed only with $O(n^2 log(n))$ operations, where n is the number of vertices of S; however, its approximation (Hilaga et al., 2001) runs in $O(knlog(n))$ operations, where k is a constant that represent a number of basis for the function evaluation. The approximation of the geodesic distance using the Dijkstra algorithm makes this function sensitive to the vertex distribution. To avoid this problem a uniform remeshing is required.

Moreover, the underlying slicing mechanisms has to be handled with care:

for example, if only a too small number of contour levels is considered, holes completely contained in the interior of a single region are missed.

This problem is related to the slicing frequency, and allows the user to get rid of little features that are considered irrelevant. Nevertheless, if topological accuracy is required, the problems can be easily overcome with the insertion of an additional number of contours into regions having holes (these regions can be always detected locally in each slice using the Euler, see (Attene et al., 2003) for details). Therefore, even if the contours may be non uniformly distributed on the domain of f, the ERG will correctly represent the topology of the surface.

The value of f and a geometric descriptor are associated to each node in the simplified ERG. The attributes used in the literature mainly associate a set of local geometric attributes to each shape slice. In our approach we move from a local description of the surface slice to a more general representation of the model sub-parts, based on the assumption that the larger the model portion associated to a node is, the more relevant the node should be. Since the ERG is directed, each node is associated to a sub-graph, and this sub-graph defines a sub-part of the shape. For leaf nodes, whose sub-graph is empty, we consider only the slice of the shape that correspond to them. Once sub-parts have been associated to each node, we use the spherical harmonic analysis of the sub-part to describe its geometry. Spherical harmonic analysis has been defined in (Kazhdan et al., 2003), and this descriptor is rotation and scale invariant and stores the shape distribution of each shape sub-part. Therefore, each node is indexed using a matrix, whose values depend on the spherical harmonic values of the related sub-part.

In figure 4, we show the shape description of the linkage model (see figure 3). The ERG structure is represented by the graph, and each node is depicted with the sub-part it generates. Since the holes in the model are not symmetric with respect to the center of mass, the sub-parts associated to the two leaf nodes slightly differ.

In addition, mainly for visualization purposes, we also store the coordinates of the centroid of the region corresponding to the node and the type of the node (i.e. maximum, minimum or saddle). Finally, the number of regions crossed during the edge construction is also associated to each edge of the ERG, and this value reflects the length of the edge before the simplification step.

The structural representation provided by our shape descriptor may differ from the intuitive notion of shape structure but, since it is related to the mathematical properties of the mapping function, it objectively reflects these properties and discard the other ones acting as a filter for the following matching operations.

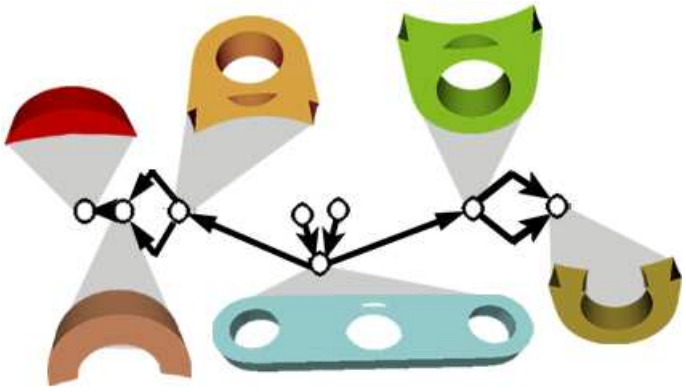

Fig. 4. The ERG representation of the model in figure 3 and some of the model sub-parts associated to graph nodes.

4 Comparison by Structural Descriptors Matching

The sub-part correspondence between two objects is obtained by matching the directed attributed graphs corresponding to the two object's structural descriptors. Techniques for exact and inexact graph matching have been topic of research for many years, and several techniques are available: recently, in (Demirci et al., 2004) the problem of inexact directed graph matching has been reduced to the problem of geometric point matching. In (Messmer and Bunke, 1998), the authors defined an algorithm for the error correcting sub-graph isomorphism (ECSI) detection; in (Cordella et al., 2004) a state space representation algorithm for the maximum common sub-graph extraction among large graphs was presented. The framework proposed in (Biasotti and Marini, 2005; Marini et al., 2005; Marini, 2005) formalizes the enumeration of all common sub-graphs of two graphs in a way that makes it easy to plug heuristics in it which may achieve different approximations of the optimal solution, according to the needs of the specific case. The matching algorithm proposed in this paper is a specialization of the method described in (Marini et al., 2005; Marini, 2005) to partial graph matching.

Given two objects and their structural descriptors, the sub-part correspondence between them can be represented by a bijective function between nodes and edges of the two structural descriptors. As previously stated, there are different ways to build such a function: for example, graph isomorphism, subgraph isomorphism, common subgraph and error tolerant graph isomorphism (see the definitions 3, 4, 5 in appendix A). The existence of a graph isomorphism implies that the two graphs must be identical, while, given two graphs $\mathcal{G}1$ and $\mathcal{G}2$, the subgraph isomorphism, implies that $\mathcal{G}1$ has to be identical to a subgraph of $\mathcal{G}2$. These are too strong conditions that can not be satisfied when the goal is the evaluation of similarity or sub-part correspondence between non identical objects. The strong requirements of the graph and subgraph isomorphism can be relaxed using a weaker similarity measure based

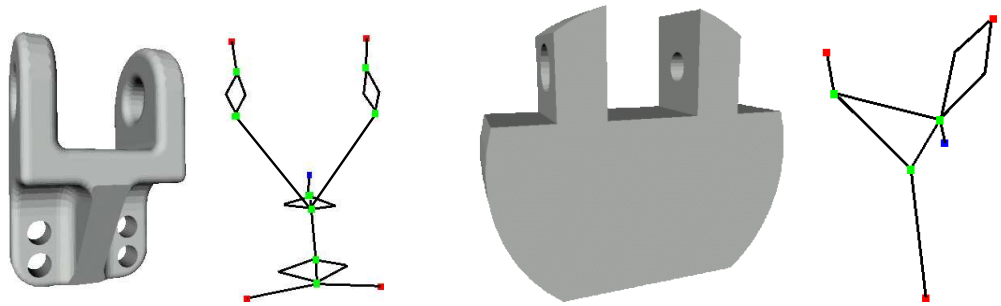

Fig. 5. Two mechanical objects with their structural graphs.

on the notion of common subgraph and error tolerant subgraph isomorphism (see definitions 5 and 7 in appendix A). ¿From an intuitive point of view, comparing two structural descriptors means constructing the most suitable common sub-graph: the wider the common sub-graph is, the more the two structural descriptors are similar. The word *suitable* has been intentionally used because more than one common sub-graph can be defined, but not all the common sub-graphs provide the same information; moreover, the mapping between nodes and edges has to take into account the differences between the attributes involving the notion of error tolerant matching. For example in figure 5 two mechanical objects are shown together with their graphs. Even if the two models have different overall shape, the expected result should produce the correspondence between the two protrusions in the upper part of the models. In figure 6 two different common subgraphs between the two shape descriptors of figure 5 are depicted: (b) represents a common sub-graph whose node mapping is not meaningfull because nodes corresponding to dissimilar sub-parts have been mapped together, while in (a) the common sub-graph represented is smaller than the former but more meaningful, because similar parts of the two objects have been correctly recognized and mapped (a correspondence between the protrusions of the two models has been identified); moreover, dissimilarities have been highlighted (the sub-parts connecting the protrusions have been recognized as dissimilar).

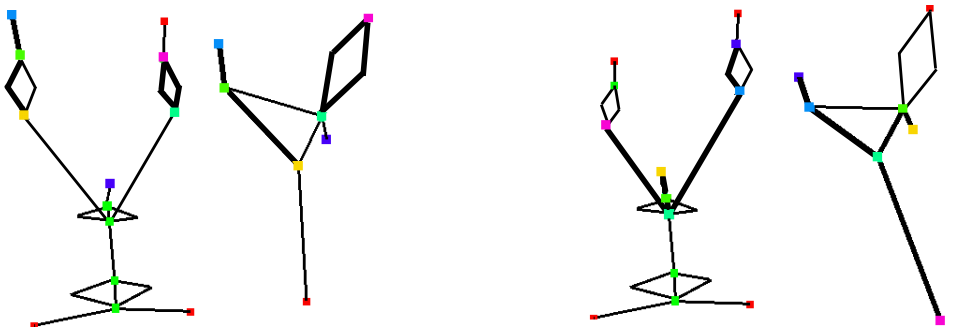

(a) (b)

Fig. 6. Two common sub-graphs between the graphs of two mechanical parts. Nodes having the same colors are mapped together. Thick edges represent edge mapping

According to the notation adopted in (Marini et al., 2005) and the definition shown in appendix A, a graph $\mathcal{G}$ is a common sub-graph of $\mathcal{G}_1$ and $\mathcal{G}_2$ if there exists a sub-graph isomorphism from $\mathcal{G}_1$ to $\mathcal{G}$ and from $\mathcal{G}_2$ to $\mathcal{G}$. A maximal common sub-graph is a common sub-graph that can not be extended to another sub-graph by the addition of nodes or edges. A maximum common sub-graph of $\mathcal{G}_1$ and $\mathcal{G}_2$ is a common sub-graph $\mathcal{G}$ such that there exists no other common sub-graph having more nodes than $\mathcal{G}$. The maximum common sub-graph in not necessarily unique. The output of the matching process, devoted to the recognition of the similar sub-parts, should be the largest maximal common sub-graph that minimizes the geometric and the structural differences of the two objects. The proposed matching algorithm can be synthetically described by the two following steps:

(1) enumerate all the possible mappings m among the nodes of the two graphs $\mathcal{G}_1$ and $\mathcal{G}_2$.
(2) for each listed mapping m, compute the common sub-graphs of $\mathcal{G}_1$ and $\mathcal{G}_2$ obtainable by expanding the mapping m.

The step 2 expands the input mapping m as much as possible while respecting the definition of common sub-graph. This algorithm is optimal in the sense that it returns all possible common sub-graphs, but it has an exponential computational complexity. For this reason, heuristic techniques are used to approximate the largest maximal common sub-graphs of the two input graphs. The involved heuristics are based on the attributes of edges and nodes, on reasoning about the graph structure and on devising an approximation which makes the structural shape matching robust to structural noise of the graph.

In general, running the algorithm on a subset of the possible initial mappings, instead of all the possible mapping, yields an approximations of the output common sub-graph set, and heuristics can be used to select the best candidate initial mappings. Depending on the attributes and on the topology of the graph, indeed, we may deduce that some nodes are more relevant than others. The initial mappings can be achieved taking into account the direction of the edges. Since the considered input graph $\mathcal{G} = (\mathcal{V}, \mathcal{E}, \mu^{\mathcal{V}}, \mu^{\mathcal{E}})$ is directed and acyclic, each node $v \in \mathcal{V}$ identifies a sub-graph $\mathcal{G}' = (\mathcal{V}', \mathcal{E}', \mu^{\mathcal{V}'}, \mu^{\mathcal{E}'})$ induced by $\mathcal{V}'$, where $\mathcal{V}'$ is the set of nodes with v as ancestor included v itself. The notion of node relevance can be captured by the sub-graph associated to the node: a large sub-graph corresponds to a large amount of structural and geometric information and then to a more relevant articulated object sub-part. This concept of relevance can be used to drive the selection of the best initial candidates for the expansion process. Given a graph $\mathcal{G} = (\mathcal{V}, \mathcal{E}, \mu^{\mathcal{V}}, \mu^{\mathcal{E}})$, for each node $v \in \mathcal{V}$ and the related sub-graph induced by v, $\mathcal{G}_v = (\mathcal{V}_v, \mathcal{E}_v, \mu^{\mathcal{V}_v}, \mu^{\mathcal{E}_v})$, the node relevance can be defined as:

$$Rel_{\mathcal{G}}(v) = |\mathcal{V}_v| \; w_{\mathcal{G}}(v) \tag{1}$$

where $|\mathcal{V}_v|$ is the number of nodes of the subgraph $\mathcal{V}_v$ and $w_{\mathcal{G}}(v)$ is a weight varying on the range $[0, 1]$ and depending on the attributes of nodes and edges of the sub-graph $\mathcal{G}_v$ associated to the node v. The weight captures the meaning of the object sub-parts represented as nodes and edges of the graph: a complex sub-graph, with many nodes and edges but representing small object sub-parts, is less relevant of a simple sub-graph, with few nodes and edges but representing a big object sub-part. A formal definition of $w_{\mathcal{G}}(v)$ is the following:

$$w_{\mathcal{G}}(v) = \frac{\sum_{e \in \mathcal{E}_v} \mu^{\mathcal{E}_v}(e)}{\sum_{e \in \mathcal{E}} \mu^{\mathcal{E}}(e)} \tag{2}$$

where $\sum_{e \in \mathcal{E}_v} \mu^{\mathcal{E}_v}(e)$ is the size of the object sub-part associated to the sub-graph $\mathcal{G}_v$ computed through the attributes associated to each edge ($\mu^{\mathcal{E}_v}(e)$), while $\sum_{e \in \mathcal{E}} \mu^{\mathcal{E}}(e)$ is the size of the whole object computed as sum of the attributes of all the edges of the graph. Starting from the equation 1, the set of the relevant nodes, $R_{\mathcal{G}}$, has been defined through the notion of average node relevance as shown in the equations 3 and 4:

$$anr_{\mathcal{G}} = \frac{\sum_{v \in \mathcal{V}} Rel_{\mathcal{G}}(v)}{|\mathcal{V}|} \tag{3}$$

$$R_{\mathcal{G}} = \{v \in \mathcal{V} \mid Rel_{\mathcal{G}}(v) \geq w_r \; anr_{\mathcal{G}}\} \tag{4}$$

where $anr_{\mathcal{G}}$ is the average node relevance of the graph and w_r is a user-defined weight depending on the application context.

Another useful heuristic has been defined associating to the pair of nodes (v_1, v_2) the information about how much the common sub-graph would expand with the addition of that pair. A distance function d between two nodes v_1 and v_2 retrieve this information. The distance $d(v_1, v_2)$ involves node and edge attributes and the approximation of the structure of the sub-graphs related to v_1 and v_2. It is defined as:

$$d(v_1, v_2) = \frac{w_1 G_S + w_2 St_S + w_3 Sz_S}{3} \tag{5}$$

where G_S, St_S and Sz_S are real numbers, $G_S,\ St_S,\ Sz_S \in [0, 1]$, representing the geometric, structural and size similarity between the sub-graphs associated to the nodes and in consequence between the objects sub-parts.

G_S compares the geometric signatures associated to v_1 and v_2. The signature of each node is obtained decomposing the sub-part surface into a collection of functions defined on concentric spheres and using spherical harmonics to discard orientation information for each one, (Kazhdan et al., 2003).

The similarity St_S between the sub-graph structures is defined as:

$$St_S = \frac{\overline{in} + \overline{out} + \overline{sub_n} + \overline{sub_in} + \overline{sub_out}}{5}, \tag{6}$$

where

$$\overline{X} = \frac{|X(v_1) - X(v_2)|}{max(X(v_1), X(v_2))}$$

in and *out* represent the indegree and the outdegree of the two nodes, *sub_n* the number of the sub-graph nodes, *sub_in* and *sub_out* the indegree and outdegree sum of the sub-graph nodes.

$Sz_S = \overline{sub_s}$, where *sub_s* is the sum of the edge attributes of the sub-graph. Sz_S evaluates the similarity between the size of the sub-parts associated to nodes, where the size corresponds to the sum of the geometric attributes of the sub-graph edges as discussed in section 3.2.

Finally, the three weights w_1, w_2 and w_3 belong to the range $[0, 1]$ and combine the three components of d: depending on the application context, for example, geometry may be more important than structure or vice-versa.

In the listings 1 and 2 a brief description of the algorithm pseudocode shows how the expansion process produce the common sub-graph starting from the initial set of relevant nodes, (Marini et al., 2005). The set of relevant nodes

Listing 1. The initial mapping procedure

```
Initial_Mapping(G1, G2, M)
{
  Relevant_Nodes(G1, RG1);
  Relevant_Nodes(G2, RG2);
  for each node v1 of RG1
    for each node v2 of RG2
      Add((v1, v2), M);
}
```

`RG` (see listing 1) is computed by the procedure `Relevant_Nodes(G,RG)` as defined in the equation 4, and the set of the initial nodes mapping `M` is obtained combining all the relevant graph nodes as shown by the procedure `Initial_Mapping(G1, G2, M)` of the listing 1. The node pairs belonging to `M` are ordered with respect to d; then, the function `Pop` extracts the candidate node pair with the smallest value of d, while the statement `Check` between the edges `e1` and `e2`, guarantees the construction of the common sub-graph `CS` is correct with respect to the definition of common subgraph (definition 5

Listing 2. The comparison procedure

```
Match(G1, G2, CS)
{
 Initial_Mapping(G1, G2, M);
 while(M Not Empty){
  c = (v1, v2) = Pop(M);
  e1 = (Parent(v1), v1);
   e2 = (Parent(v2), v2);
   if(Mapped(v1) and Mapped(v2))
    if(Check(e1, e2)){
     Add((e1, e2), CS);
   }else
   if(Not Mapped(v1) and
      Not Mapped(v2)){
    Add(c, CS);
    Add((e1, e2), CS);
   }
  Update(CANDIDATES, c);
  }
 }
```

of appendix A). `Updates` adds new node pairs to `M` combining all the nodes outcoming from `v1` and `v2`. The initial mapping among relevant nodes makes the algorithm robust with respect to structural noise allowing the construction of a not necessarily connected common sub-graph. This last characteristic of the matching process, enables the recognition of similar sub-parts even if the overall objects shape/structure is dissimilar.

5 Results

In this section some experimental results on manufactured models are provided and discussed. The experiments have been performed on about 250 models, collected into several web repositories. About 190 CAD models, which comes from the National Design Repository at Drexel University[1] have been uniformly remeshed to perform an accurate evaluation of the geodesic function. Other manufactured models have been considered from the AIM@SHAPE repository[2] and from the Image-based 3D Models Archive[3]. Figure 7 shows some examples of models belonging to the database.

[1] http://www.designrepository.org
[2] http://shapes.aim-at-shape.net
[3] http://www.tsi.enst.fr/3dmodels

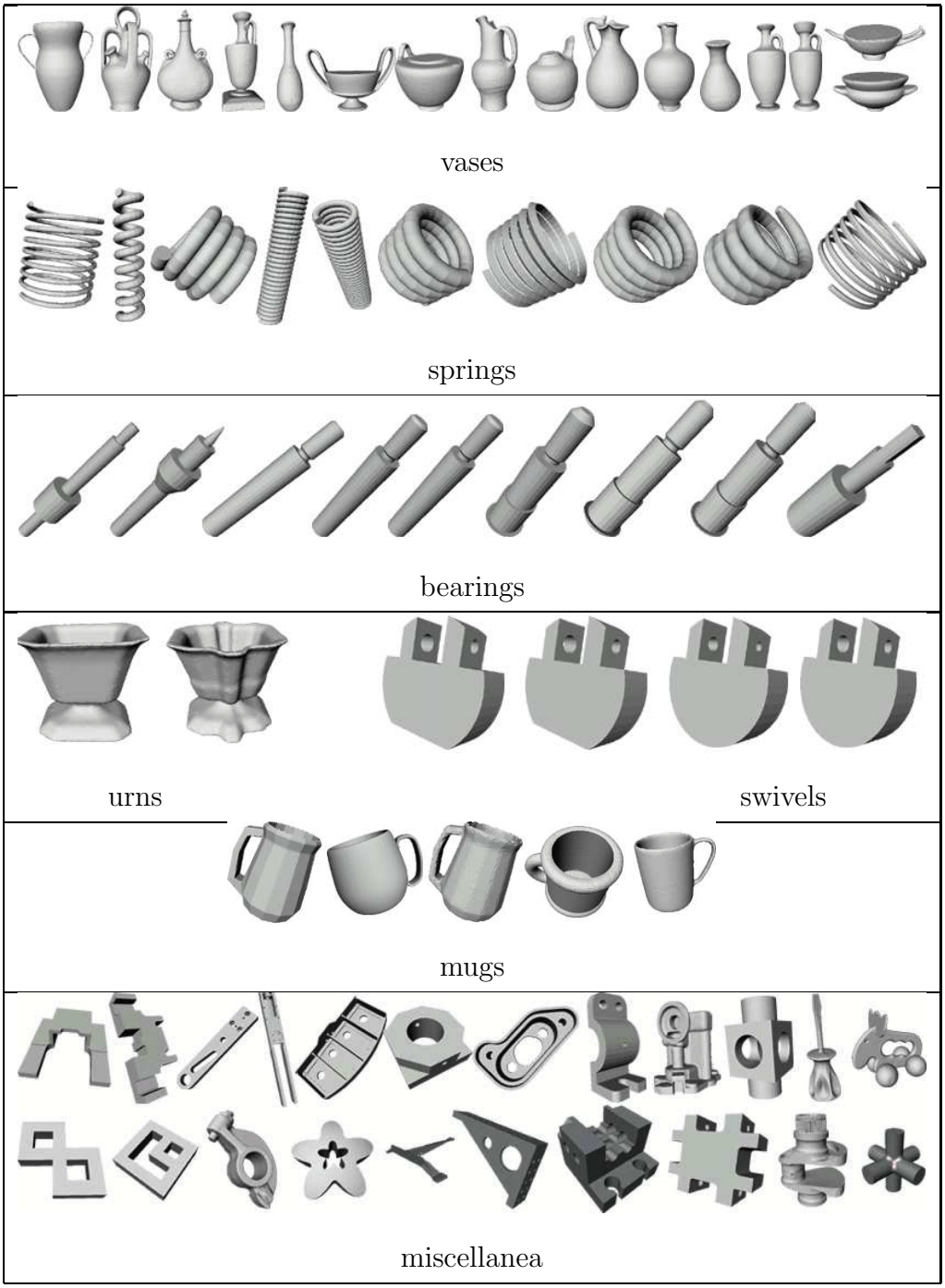

Fig. 7. Some models of our database.

As described in the sections 3 and 4, the structural descriptor captures the relevant parts of the models and encodes them as nodes and edges of a graph. The graphs associated to two objects are compared through the algorithm described in section 4 and the correspondence between the nodes and edges that represent the common sub-graph is found. The common sub-graph (may be not connected) identifies the sub-parts of the objects that are similar, while the parts of the graphs that do not belong to the common sub-graph highlight the

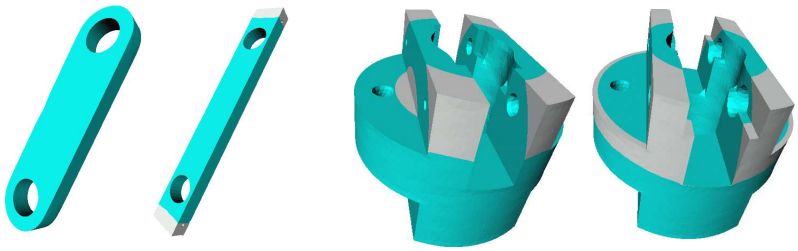

(a) (b) (c) (d)

Fig. 8. The sub-part correspondence between the models (a) and (b) is shown associating the same color to regions that are matched. Regions in grey are not matched. Similar results for (c) and (d).

dissimilarities between the two models. The following convention is adopted to show the results: the sub-part correspondence between two models is represented by coloring the matched sub-part of each model with the same color, and different colors represent different connected components of the common subgraph. When the common sub-graph corresponds to the whole graph of both the compared graphs, the color associated to each node reproduces the matched sub-parts of the two models as shown in figure 9.

In order to validate the approach proposed in this paper, the experiments are performed and discussed for sub-part correspondence, global matching and finally on partial matching.

5.1 Sub-Part Correspondence

In figure 8 the performance of the method for detecting the sub-part correspondence is tested. Although the overall shape of the models (a) and (b) (resp. (c) and (d)) is similar, the models differ for some small geometric details: the tips of (a) are rounded, while in (b) are squared; and the slots in the upper part of (c) differ from that of (d). In both the cases, the partial matching process correctly recognizes the correspondence among similar sub-parts, while if some shape features have no correspondence in the other models, they are not mapped at all, as shown by the grey parts of the figure 8. In figure 9 other two models with the same overall shape are shown. The models and their structural descriptors are shown in figure 9(a). The correspondence between the two graphs and the relative node mapping are shown in figure 9(b). Similar sub-parts of the two models are in figure 9(c). The differences between the two models are minimal but the two graphs describing them have an isomorphic structure. In this case the sub-parts corresponding to the nodes `c` and `c1` as well as `d` and `d1` are mapped even if they have small differences, but these differences can be recognized looking at the dissimilarity values, provided by

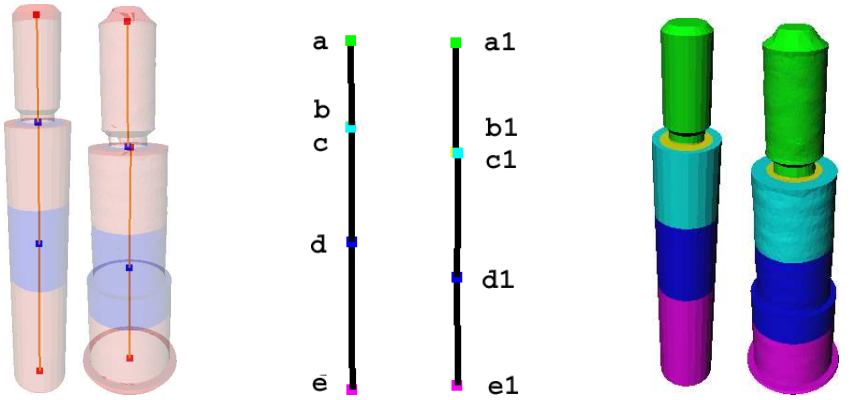

(a) (b) (c)

Fig. 9. The two models and their graphs (a). The node correspondence is represented by nodes with the same color (b), and by regions of the same color.

the algorithm (see section 4):

$$\begin{aligned} &a \longrightarrow a1 : 0.0308798 \\ &b \longrightarrow b1 : 0.0131474 \\ &c \longrightarrow c1 : 0.0559334 \\ &d \longrightarrow d1 : 0.0988876 \\ &e \longrightarrow e1 : \ 0.146666 \end{aligned} \tag{7}$$

From (7) it is easy to perceive that the most dissimilar sub-parts correspond to the node pairs e $\longrightarrow$ e1 and d $\longrightarrow$ d1.

Even though the global characteristic are analogous, the main difference between the two models shown in the figures 10 concern the two small holes in the rear part of (b) that are not present in (a). The comparison process recognizes the presence of the two holes and highlights the difference between the two models (figure 10(c)). The grey part (not colored) in the right part of figure (c) identifies the sub-part of (b) that is not mapped with any sub-part of (a). The comparison process between the two structural descriptors produces a non connected common sub-graph made of two connected components separated by the non matched sub-part (in grey). In figure (c), the two connected components are shown with different colors (blue and green).

5.2 Global Matching

The capability of the comparison process to solve the sub-part correspondence problem positively influences the results of the global matching for shape re-

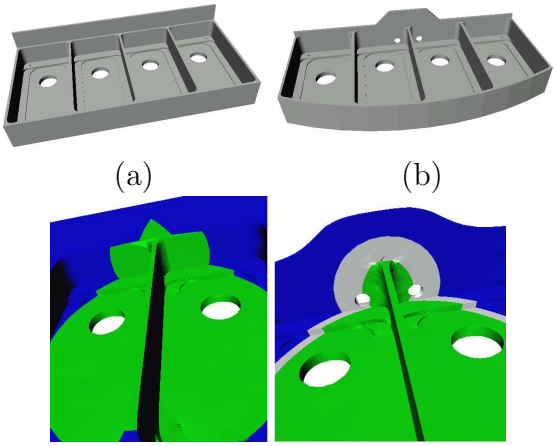

(a) (b)

(c)

Fig. 10. The model (b) has two small holes on its rear part that do not have any counterpart in the model (a). A detail of the correspondence between sub-parts the two models is shown in (c): the grey region identifies the difference between the two models.

trieval applications. The similarity estimation between two objects can be obtained by considering the size of the common subgraph with respect to the size of the two graphs and the similarity distance between the nodes belonging to the common subgraph, as computed by the equation (5). The distance measure between two graphs $\mathcal{G}1$ and $\mathcal{G}2$ is defined by the equation (8), and it is derived by the one discussed in (Biasotti et al., 2003b):

$$D(\mathcal{G}1, \mathcal{G}2) = 1 - \frac{\sum_{v \in \mathcal{G}}(1 - d(\psi_1(v) - \psi_2(v)))}{max(|\mathcal{G}1|, |\mathcal{G}2|)} \tag{8}$$

where $\mathcal{G}$ is the common subgraph between $\mathcal{G}1$ and $\mathcal{G}2$, and ψ_1 and ψ_2 are the subgraph isomorphisms from $\mathcal{G}$ to $\mathcal{G}1$ and from $\mathcal{G}$ to $\mathcal{G}2$, as described in the definition 5 of appendix A.

Figure 11 shows the results obtained experimenting the matching process on a database containing mechanical parts, animals, humans, fornitures and archaeological objects.

The experiments has been performed by considering the center of mass distance and the integral geodesic function, (Biasotti et al., 2003a). A uniform subdivision of the function image, $[f_{min}, f_{max}]$, is considered and the contour levels (see section 3) are inserted in correspondence of these function values. In particular the number of intervals in $[f_{min}, f_{max}]$ is named "resolution" of the graph. Two resolutions has been choosen to test the different behaviour with respect to the level of detail used to analyze the object. In figure 11(a) and (b) the center of mass distance has been used with resolutions 16 and 64 respectively, the same resolutions are also used for the integral geodesic

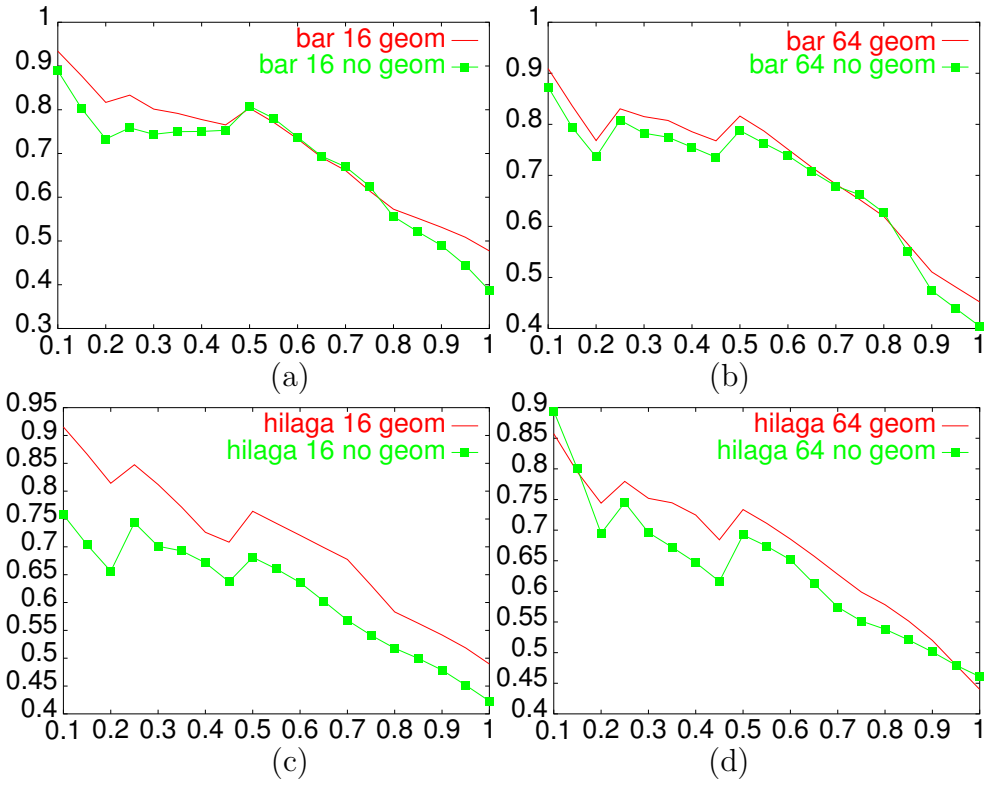

Fig. 11. The precision-recall diagrams on the ERG computed with the center of mass distance with resolution 16 (a) and 64 (b), and with the integral geodesic distance with resolution 16 (c) and 64 (d). The tests has been performed considering structural and geometrical information ("geom") and only structure ("no geom").

function in the figures (c) and (d). The diagrams show the results obtained by executing the matching algorithm consdering structure combined with geometry through the node distance notion defined in equation (5) (titled in the diagrams as "geom"), and also considering only structure and not geometry information, re-definig the distance $d(v_1, v_2) = St_S$, where St_S is defined in the equation (6). In this case the title of these diagrams is "no geom".

The figure 11 shows that the use of geometrical information, coupled with the structural information encoded in the descriptor improve the performance of the matching process for both the descriptors. However, the diagrams represented in (c) and (d) show that the performance of the graph based on the integral geodesic distance highly influenced by the geometrical information associated to the graph, while the graph based on the distance from the center of mass is less sensible to geometry.

Finally figure 12 summarizs the performance of the previous tests and the diagram shows that the distance from the center of mass function with resolution 64 perform better than the geodesic one. In figure 13 some examples of shape retrieval results are shown.

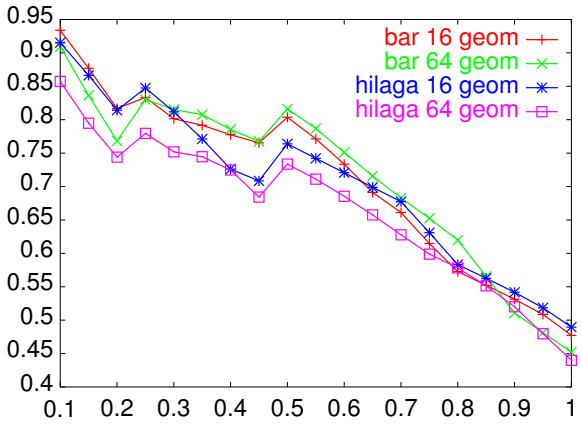

Fig. 12. Precision recall diagrams of the ERGs based on the centre of mass distance function and integral geodesic function represented with resolution 16 and 64, and considering both structural and geomettrical information during the similarity estimation.

5.3 Partial Matching

An example of partial correspondence among models having different overall appearance is given in figure 14. In this case the models differ both in structure and geometry but they have similar sub-parts: even if the two big protrusions are not similar from a geometric point of view they have similar structure. The coupling of geometry and structure pursued by our algorithm correctly map these sub-parts. On the contrary, the central parts of the models are different both in structure and geometry, thus they are not recognized as similar sub-parts.

Once the similar sub-parts have been recognized, the node mapping between the two structural descriptors automatically provides a way for mapping the model sub-parts associated to the graph nodes. In figure 15(a) the two models of figure 14 are shown along with their graphs, while in figure 15(b) the two graphs has been matched and the node and edge correspondence is represented. According with such a correspondence, the figure 15(c) shows the more detailed sub-part correspondence.

Figure 16 shows two examples where a whole model is a sub-part of another one. Even if the two shapes of (a) and (b) are dissimilar, the elongated part shown in (b) is correctly recognized as sub-part of the model (a), because the structural descriptor of (a) correctly characterizes both the geometry and the structure of the sub-part that identifies the long part of the screwdriver. The same happens for the models (c) and (d). In this case, the sub-part containing the four holes of the model (c) is not mapped to any part of themodel (d).

Other examples concerning the sub-part correspondence between 3D models are shown in figure 17. The cubes in figure (a) have two blind-holes with

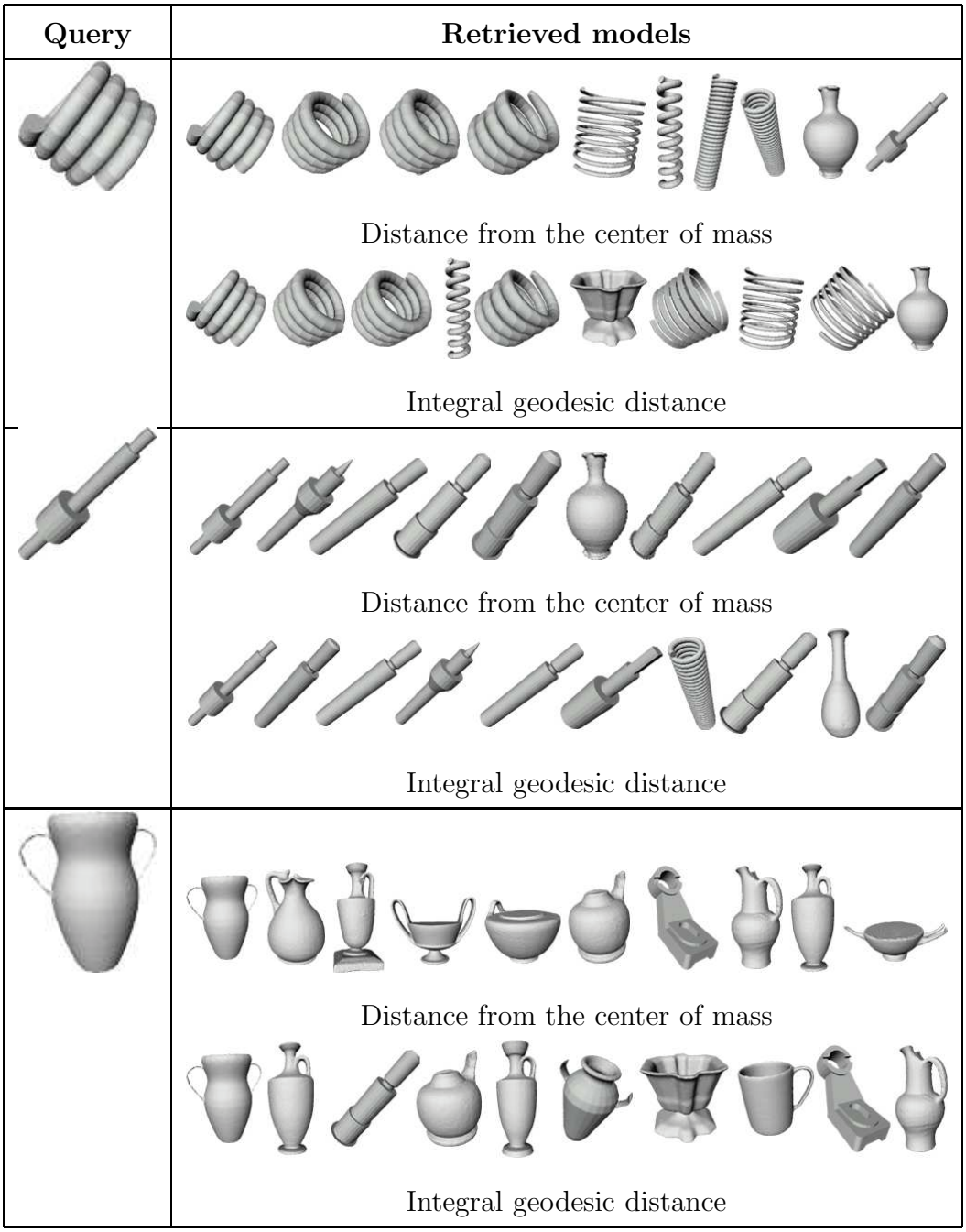

Fig. 13. Experimental results of the global matching problem.

different shape and the structural descriptor encodes these differences and the comparing algorithm highlights them; the left model in (b) has a deep squared pocket on one of its faces, while the blend region in the two models in (c) significantly differ. In both the cases the similar and the dissimilar sub-parts are correctly recognized. The two springs of figure (d) have different spatial distribution but the structure is the same, as well as models in (e), (f) and (g). The models in (h) have the same structure but the sub-parts have different proportion. This produces a difference both in structure and in geometry.

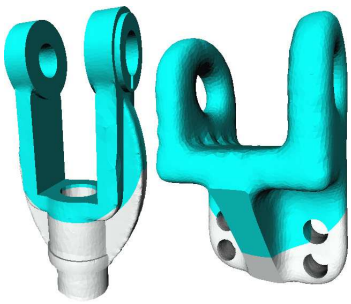

Fig. 14. The correspondence between the sub-parts of the two models is highlighted by the color.

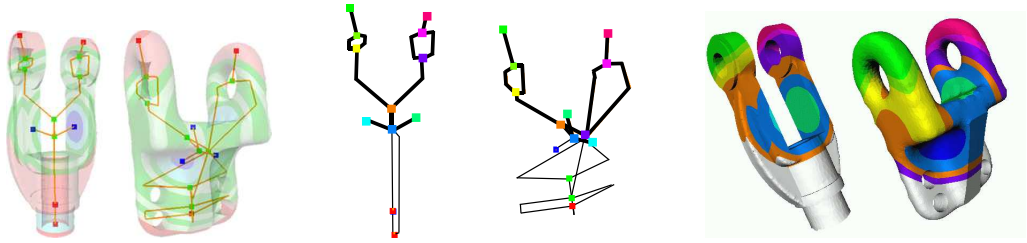

(a) (b) (c)

Fig. 15. Two models are shown together with their graphs (a). The correspondence between the two graphs is represented by nodes with the same colors (b). The node correspondence between the two graphs is reproduced on the two models, respecting the colors associated to the nodes (c).

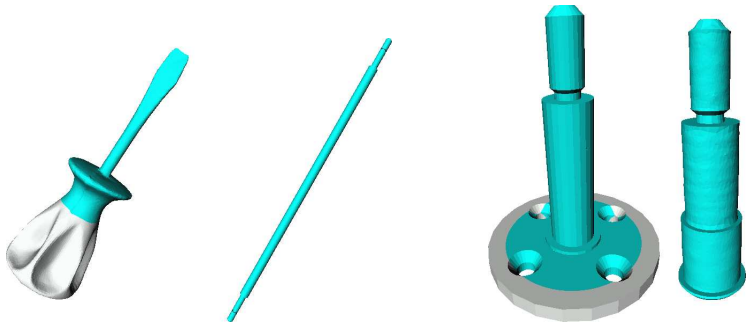

(a) (b) (c) (d)

Fig. 16. The models (b) and (d) are recognzed as sub-parts of the models (a) and (c) respectively.

6 Conclusion and Future Work

In this paper we have presented a new method for measuring the similarity and recognizing sub-part correspondences of 3D shapes, based on the coupling of global and local descriptors of geometry and topology. The proposed framework offers an effective solution to the problem of searching and retrieval in general, and, since the matching relies on structural descriptions, the system is particularly suitable for sub-part correspondence. As shown in figures 17 and

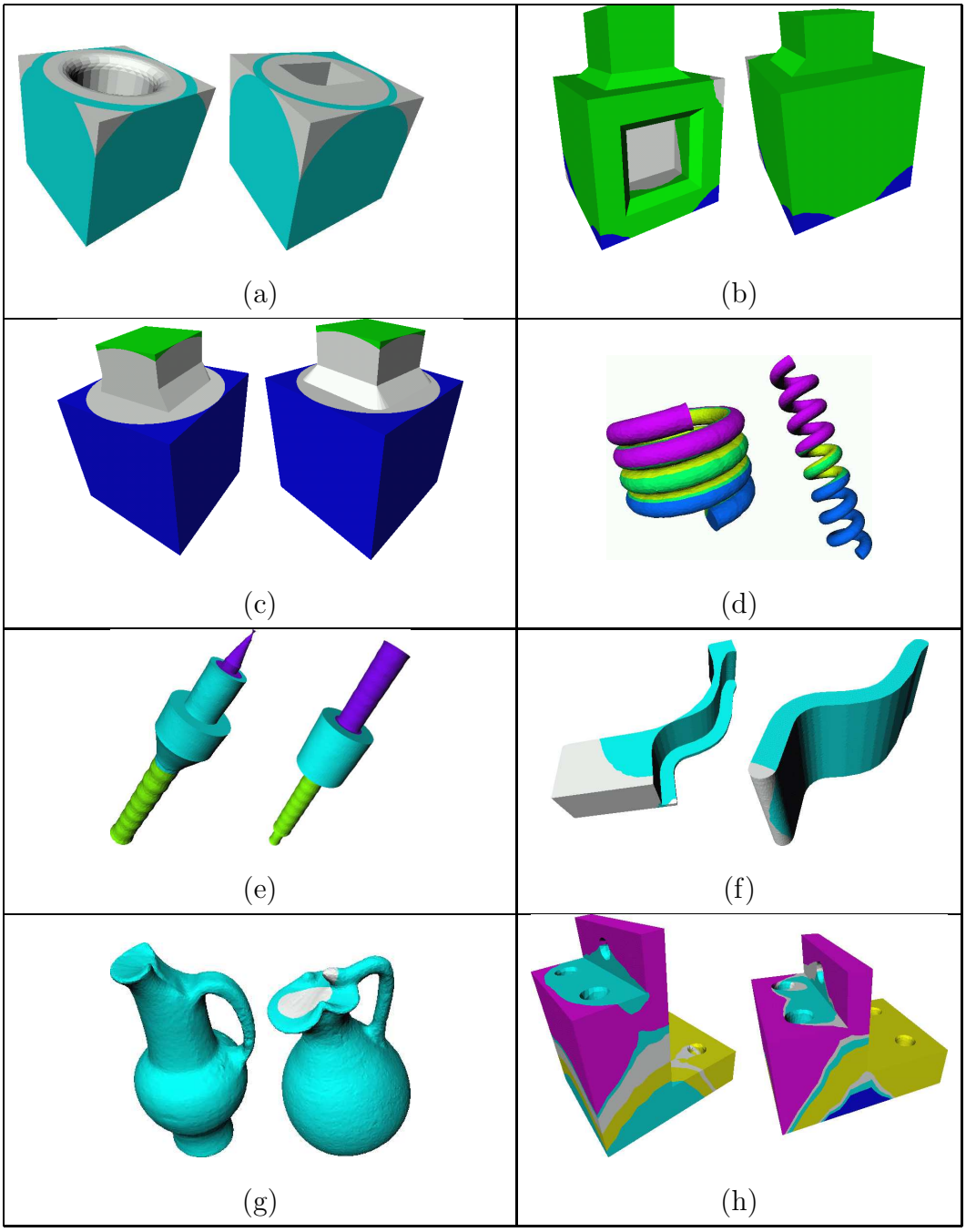

Fig. 17. Some examples of sub-part correspondences.

16, this coupling is advantageous for comparing models having similar overall shape and structure, as well as only common sub-parts.

We demonstrated that structure-based matching can improve the retrieval performance in terms of both functionalities supported (i.e., partial and sub-part correspondences) and the variety of shape descriptions that can be used to tune the retrieval with respect to the context of application.

About the shape descriptor used, one might argue that the graph encodes the relevant characteristics of the model but the sub-parts of the object associated to the graph nodes do not necessarily correspond to standard CAD features. We have seen from the experiments, however, that the characteristics detected by the mapping functions contribute to localize important CAD features as well. It is interesting to point out that, depending on the choice of f, the ERG and the associated shape descriptor detect relevant morphological characteristics like protrusions, pockets, branchings, slots, narrowings and involutions, that users may combine with other information and vary according to their desiderata. Having selected the most appropriate mapping function, the shape segmentation and the construction of the associated descriptor is fully automatic and does not require any user interaction. In other words, the selection of f defines the features that do not need to be pre-defined and limited to a given set of primitives. Also, the use of the geometric attributes to code the node sub-parts, naturally provides a hierarchical description of the most relevant features. We want to underline, however, that any other suitable skeletal structure could be used, provided that it can be coded as an attributed, directed and acyclic graph.

The flexibility related to the choice of f may be regarded as an advantage over previous methods: the method described in (Huber et al., 2004) works on an arbitrary object segmentation (the model is always split into three parts) independently of the shape object complexity; the method proposed in (Fan et al., 1989) produces an automatic and structural subdivision of the object surface but it works only on simple surfaces where shape discontinuities are present and easily recognized; the object segmentation in (Ruiz-Correa et al., 2003; Funkhouser et al., 2004) is obtained by user interaction.

In the framework proposed is the ERG can be used only to analyse and code connected models, that is, polygon soups are not tractable. However, this doas not constitute a problem for designing CAD models, that usually are complete and valid topological models.

As future work, we are planning to extend the approach to other kinds of representations used for free form 3D object models. We are also trying to combine it with other approaches, to contribute to the design of multistep, multimodal search engines for 3D models.

Acknowledgement

This work has been partially supported by the EU Newtwork of Excellence "AIM@SHAPE" [4] . Moreover, the authors would like to thank Remco Veltkamp and Thomas Funkhouser for the helpful discussions on this topic.

A Basic Definitions on Graphs

Definition 1 (Attributed graph) *An attributed graph $\mathcal{G}$ is given by a quadruple $G = (V, E, \mu_V, \mu_E)$, where V is a set of nodes, E is the set of the graph edges, $\mu_V : V \rightarrow A_V$ and $\mu_E : E \rightarrow A_E$ are the node and the edge attribute functions, with A_V, A_E sets of node and edge attributes of G.*

Definition 2 (Attributed sub-graph) *A sub-graph S of G is a quadruple $(V_S, E_S, \mu_{V_S}, \mu_{E_S})$, where $V_S \subseteq V$, $E_S \subseteq E$, μ_{V_S} and μ_{E_S} are induced by μ_V and μ_E, respectively.*

Definition 3 (graph isomorphism) *is a bijective function $f : \mathcal{V}_1 \rightarrow \mathcal{V}_2$ such that:*

(1) $\mu^{\mathcal{V}_1}(v) = \mu^{\mathcal{V}_2}(f(v)),\ v \in \mathcal{V}_1$.
(2) for all the edges $e_1 = (v_1, v_1') \in \mathcal{E}_1$, there exists an edge $e_2 = (f(v_1), f(v_1')) \in \mathcal{E}_2$ such that $\mu^{\mathcal{E}1}(e_1) = \mu^{\mathcal{E}_2}(e_2)$. Moreover, for all the edges $e_2 = (v_2, v_2') \in \mathcal{E}_2$, there exists an edge $e_1 = (f^{-1}(v_2), f^{-1}(v_2')) \in \mathcal{E}_1$ such that $\mu^{\mathcal{E}_1}(e_1) = \mu^{\mathcal{E}_2}(e_2)$.

If a graph is not attributed, the condition 1 and the equality between the edge attributes in the condition 2, are not necessary.

Definition 4 (sub-graph isomorphism) *If $f : \mathcal{V}_1 \rightarrow \mathcal{V}_1'$ is a graph isomorphism between the graph $\mathcal{G}_1$ and $\mathcal{G}'$, and $\mathcal{G}'$ is a sub-graph of $\mathcal{G}_2$, then f is called a sub-graph isomorphism from $\mathcal{G}_1$ to $\mathcal{G}'$.*

Definition 5 (common sub-graph) *A common sub-graph of $\mathcal{G}_1$ and $\mathcal{G}_2$ is a graph $\mathcal{G}$ such that there exists a sub-graph isomorphism from $\mathcal{G}$ to $\mathcal{G}_1$ and from $\mathcal{G}$ to $\mathcal{G}_2$.*

Definition 6 (maximum common sub-graph) *A maximum common sub-graph of $\mathcal{G}_1$ and $\mathcal{G}_2$, denoted as $\mathcal{MCS}_{\mathcal{G}_1,\mathcal{G}_2}$ is a common sub-graph $\mathcal{G}$ such that there exists no other common sub-graph having more nodes than $\mathcal{G}$. The $\mathcal{MCS}_{\mathcal{G}_1,\mathcal{G}_2}$ in not necessarily unique.*

[4] http://www.aimatshape.net

Definition 7 (error tolerant (sub)graph isomorphism) *Let $\mathcal{G}$ and $\mathcal{G}'$ be two attributed graphs as proposed in definition 1 and $\Delta = (\delta_1, \ldots, \delta_n)$ a sequence of graph editing operations, where a graph edit operation, δ_i, is an addition, a deletion or an attribute modification of nodes and edges, then:*

- *the* edited graph $\Delta(\mathcal{G})$ *is the graph* $\Delta(\mathcal{G}) = \delta_n(\delta_{n-1}(\ldots \ (\delta_1(\mathcal{G})) \ldots))$*;*
- *an* error tolerant graph isomorphism *is a couple* (Δ, ψ)*, where* Δ *is a sequence of editing operations such that there exists an graph isomorphism* ψ *between* $\Delta(\mathcal{G})$ *and* $\mathcal{G}'$*.*

References

Attene, M., Biasotti, S., Spagnuolo., M., 2003. Shape understanding by contour driven retiling. The Visual Computer 19 (2-3), 127–138.

Bespalov, D., Ip, C. Y., Regli, W. C., Shaffer, J., 2005. Benchmarking cad search techniques. In: Proceedings of the 2005 ACM symposium on Solid and physical modeling. pp. 275–286.

Bespalov, D., Regli, W. C., Shokoufandeh, A., September 2003a. Reeb graph based shape retrieval for CAD. In: Proceedings of the 2003 ASME Design Engineering Technical Conferences. ASME, Chicago, Illinois.

Bespalov, D., Shokoufandeh, A., Regli, W. C., Sun, W., June 2003b. Scale-space representation of 3D models and topological matching. In: Proceedings of the 8^{th} ACM Symposium on Solid Modeling and Applications. ACM Press, Seattle, Washington, pp. 208–215.

Bespalov, D., Shokoufandeh, A., Regli, W. C., Sun, W., Sep 2004. Local feature extraction using scale-space decomposition. In: ASME Design Engineering Technical Conferences, Computers and Information in Engineering Conference Conference (DETC 2004-57702). ASME Pres.

Biasotti, S., May 2004. Computational topology topology methods for shape modelling applications. Ph.D. thesis, University of Genova.

Biasotti, S., Marini, S., 2005. 3D object comparison based on shape descriptors. International Journal of Computer Applications in Technology 23 (2/3/4), 57–69.

Biasotti, S., Marini, S., Mortara, M., Patané, G., May 2003a. An overview on properties and efficacy of topological skeletons in shape modelling. In: Proceedings of Shape Modelling and Applications. IEEE Press, Seoul, South Korea, pp. 245–254.

Biasotti, S., Marini, S., Mortara, M., Patanè, G., Spagnuolo, M., Falcidieno, B., 2003b. 3d shape matching through topological structures. In: Proc. of DGCI. Vol. 2886 of Lecture Notes in Computer Science. pp. 194–203.

Biederman, I., 1987. Recognition-by-Components: A theory of human image understanding. Phicological Review 94, 115–147.

Blum, H., 1967. A transformation for extracting new descriptors of shape. In:

Whaten-Dunn, W. (Ed.), Proceedings of the Symp. Models for Perception of Speech and Visual form. Cambridge MA: MIT Press, pp. 362–380.

Cole-McLaughlin, K., Edelsbrunner, H., Harer, J., Natarajan, V., Pascucci, V., 2003. Loops in Reeb Graphs of 2-Manifolds. In: Proceedings of the 19^{th} ACM Symposium on Computational Geometry. ACM Press, pp. 344–350.

Cordella, L. P., Foggia, P., Sansone, C., Vento, M., October 2004. A (sub)graph isomorphism algorithm for matching large graphs. IEEE Transactions on Pattern Analysis and Machine Intelligence 26 (10), 1367–1372.

Demirci, M. F., Shokoufandeh, A., Dickinson, S., Keselman, Y., Bretzner, L., May 2004. Many-to-many feature matching using spherical coding of directed graphs. In: Proceedings of the European Conference on Computer Vision. Prague, pp. 322–335.

Fan, T., G.Medioni, Nevatia, R., November 1989. Recognizing 3D objects using surface description. IEEE Transactions on Pattern Analysis and Machine Intelligence 11 (11), 1140–1157.

Funkhouser, T., Kazhdan, M., Shilane, P., Min, P., Kiefer, W., Tal, A., Rusinkiewicz, S., Dobkin, D., 2004. Modeling by example. ACM Transactions on Graphics 23 (3), 652–663.

Hilaga, M., Shinagawa, Y., Komura, T., Kunii, T. L., 2001. Topology matching for fully automatic similarity estimation of 3D shapes. In: Proc. of SIGGRAPH 2001. ACM Press, Los Angeles, pp. 203–212.

Huber, D., Kapuria, A., Donamukkala, R., Hebert, M., 2004. Parts-based 3D object classification. In: Proceedings of the International Conference on Computer Vision. Vol. Vol. 2. pp. 82–89.

Iyer, N., Jayanti, S., Lou, K., Kalyanaraman, Y., Ramani, K., 2005. Shape-based searching for product lifecycle applications. Computer-Aided Design 37 (13), 1435–1446.

Johnson, A. E., Hebert, M., 1997. Recognizing objects by matching oriented points. In: Proceedings of the IEEE Conference on Computer Vision and Pattern Recognition. pp. 684–689.

Katz, S., Leifman, G., Tal, A., September 2005. Mesh segmentation using feature point and core extraction. The Visual Computer 21 (8–10), 649–658.

Katz, S., Tal, A., 2003. Hierarchical mesh decomposition using fuzzy clustering and cuts. ACM Transactions on Computer Graphics, (Proc. of SIGGRAPH 2003) 22 (3), 954–961.

Kazhdan, M., Funkhouser, T., Rusinkiewicz, S., June 2003. Rotation invariant spherical harmonic representation of 3D shape descriptors. In: Kobbelt, L., Schröder, P., Hoppe, H. (Eds.), Proceedings of Symposium in Geometry Processing. Aachen, Germany, pp. 156–165.

Marini, S., April 2005. 3d shape similarity through structural descriptors. Ph.D. thesis, University of Genova.

Marini, S., Spagnuolo, M., Falcidieno, B., April 11-13 2005. From exact to apporximate maximum common subgraph. In: Proceedings of the 5rd IAPR -TC-15 Workshop on Graph-based Representations in Pattern Recognition.

Lecture Notes in Computer Science. Poitiers (France), pp. 263–272.
Marr, D., 1982. Vision - A computational investigation into the human representation and processing of visual information. W. H. Freeman, San Francisco.
Messmer, B. T., Bunke, H., May 1998. A new algorithm for error tolerant subgraph isomorphism detection. IEEE Transactions on Pattern Analysis and Machine Intelligence 20 (5), 493–504.
Novotni, M., Klein, R., May 2001. A geometric approach to 3D object comparison. In: Proceedings of Shape Modelling and Applications. IEEE Press, Genova, Italy, pp. 167–175.
Osada, R., Funkhouser, T., Chazelle, B., Dobkin, D., May 2001. Matching 3D models with shape distributions. In: Proceedings of Shape Modelling and Applications. IEEE Press, Genova, Italy, pp. 154–166.
Reeb, G., 1946. Sur les points singulièrs d'une forme de Pfaff complètement intégrable ou d'une fonction numèrique. Comptes Rendu de l'Academie des Sciences 222, 847–849.
Regli, W. C., Cicirello, V. A., Feb 2000. Managing digital libraries for computer-aided design. Journal of Computer-Aided Design 32 (2), 119–132.
Ruiz-Correa, S., Shapiro, L., Meila, M., October 2003. A new paradigm for recognizing 3D object shapes from range data. In: Proceedings of the International Conference on Computer Vision. pp. 1126–1133.
Shinagawa, Y., Kunii, T. L., Kergosien, Y. L., Sep. 1991. Surface coding based on Morse Theory. IEEE Computer Graphics and Applications 11 (5), 66–78.
Siddiqi, K., Bouix, S., Tannenbaum, A., Zucker, S. W., July 2002. Hamilton-jacobi skeletons. International Journal of Computer Vision 48 (3), 215–231.
Sundar, H., Silver, D., Gagvani, N., Dickinson, S., June 2003. Skeleton based shape matching and retrieval. In: Proceedings of Shape Modelling and Applications. IEEE Press, Seoul, South Korea, pp. 130–139.
Tung, T., Schmitt, F., June 2005. The Augmented Multiresolution Reeb Graph approach for content-based retrieval of 3D shapes. Int. J. of Shape Modelling 11 (1), 91–120.
Ullman, D. G., 1997. The Mechanical Design Process. McGraw-Hill, New York.
Vranič, D. V., Saupe, D., Richter, J., October 2001. Tools for 3D-Object retrieval. In: Proceedings of the IEEE 2001 Workshop on Multimedia Signal Processing. IEEE Press, Cannes, France, pp. 293–298.
Zhang, E., Mischaikow, K., Turk, G., 2005a. Feature-based surface parameterization and texture mapping. ACM Transaction on Graphics 24 (1), 1–27.
Zhang, J., Siddiqi, K., Macrini, D., Shokoufandeh, A., Dickinson, S., November 2005b. Retrieving articulated 3-D models using medial surfaces and their graph spectra. In: Proceedings of International Workshop on Energy Minimization Methods in Computer Vision and Pattern Recognition (EMMCVPR). St. Augustine, FL.